

Paper:

# Optimization of the Electrode Arrangement and Reliable Fabrication of Flexible EHD Pumps

Yumeta Seki\*, Yu Kuwajima\*, Hiroki Shigemune\*\*, Yuhei Yamada\*, and Shingo Maeda\*

\*Smart Materials laboratory, Shibaura Institute of Technology

3-7-5 Toyosu Koto-ku, Tokyo 135-8548, Japan

E-mail: {md19042, md17035, i046508, maeshin}@shibaura-it.ac.jp

\*\*Active Functional Device laboratory, Shibaura Institute of Technology

3-7-5 Toyosu Koto-ku, Tokyo 135-8548, Japan

E-mail: hshige@shibaura-it.ac.jp

[Received March 30, 2020; accepted August 12, 2020]

Soft robots have great potential to realize machines that interact and coexist with humans. A key technology to realize soft robots is soft fluidic actuators. Previously, we developed a soft pump using the electrohydrodynamics (EHD) phenomenon. EHD is a flow phenomenon, which is generated by applying a high voltage to a dielectric fluid. In this study, we developed flexible high-power-density EHD pumps. First, a pump was fabricated by a simple design with interdigitated electrodes. Second, a mathematical model was used to analyze the pressure generated per length assuming that electric fields only act between neighboring electrodes in a flexible EHD pump with interdigitated electrodes. The results were used to optimize the gap between electrodes to maximize the pressure per length. Third, we used the optimized process to fabricate multiple flexible EHD pumps. The procedure produced pumps easily and reliably. Fourth, we compared the experimental values with the analytical solutions. The good agreement confirmed that the generated pressure per unit length can be approximated in a uniform electric field between neighboring electrodes. Because our flexible EHD pump can operate even when deformed, it has potential for wearable device applications.

**Keywords:** reliable fabrication, flexible EHD pump, interdigitated electrode, finite element analysis

## 1. Introduction

Robots with soft bodies are sought after in many fields. Examples include various artificial muscles using dielectric elastomers [1, 2], suction pads using electrostatic adhesion [3], active gels [4–7], and self-folding paper robots [8, 9]. These robots realize soft and supple movements similar to living creatures because their construction is based on rubber, silicone, etc.

Fluid-pressure driven soft actuators have garnered increased attention as a key technology in soft robot re-

search. In 1980, Suzumori realized various flexible mechanisms by a pioneering combination of air pressure and rubber [10–12]. These fluid-pressure-driven soft actuators have three features that are advantageous for human-machine coexistence. (1) They are not dangerous to people. (2) They realize an adaptive motion, and (3) they do not break easily when an external force is applied. However, fluid-pressure-driven soft actuators require a large device like a compressor to generate fluid pressure, which increases the size and noise.

As robotics advance, there is an increased expectation that humans will connect seamlessly with machine systems. However, an unsolved issue is preventing devices from becoming larger or noisier. We recently reported soft fluid pumps and actuators using the electrohydrodynamics (EHD) phenomenon [13–16]. EHD is a flow phenomenon generated by applying a high voltage to a dielectric fluid. EHD pumps with various electrode shapes have been suggested [17, 18]. Atten et al. developed an EHD pump with needle-ring style electrodes. This pump realizes unidirectional flow via electric field asymmetry [19]. We developed a stretchable EHD pump with symmetrically placed electrodes. Our pump uses an injection pumping system, and the flow direction is controlled based on the polarity of the applied voltage. Cacucciolo et al. found that the generated pressure can be augmented using multiple electrodes [15].

To advance our previous research, we aim to optimize the electrode arrangement and establish a reliable fabrication method for flexible EHD pumps. When designing interdigitated electrodes, the distance between electrodes is a key parameter to determine the generated pressure of an EHD pump. In this research, we analyze a simple model of multiple-connected EHD pumps using interdigitated electrodes. Finite element analysis is used to optimize the distance between the electrodes and to maximize the pressure and flow rate per unit length generated by EHD pumps.

To investigate the relationships between the electrode arrangement, generated pressure, and flow rate, **Fig. 1** shows the fabricated flexible EHD pumps with different electrode arrangements. Additionally, we introduce cut-





Fig. 1. Photograph of a flexible EHD pump.

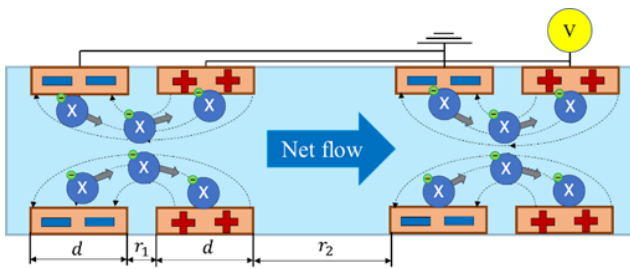


Fig. 2. Mechanism of the EHD phenomenon.

ting plotters in the electrode fabrication process to easily realize reliable and reproducible device electrodes. By adopting an adhesive elastomer in the flow path of the pump, a process to manufacture a flexible EHD pump in a short time is realized.

## 2. Mechanism

Figure 2 overviews the mechanism of our flexible EHD pump. It is a charge-injection type. Applying a high electric field (6–20 V/μm) to a dielectric liquid emits electrons from the cathode into the dielectric liquid. These electrons react with the neutral species in the dielectric liquid and generate ions. Then the ions are accelerated by the electric field and neutral species molecules move. Hence, the dielectric liquid flows inside a channel. Flexible EHD pumps produce flow toward the higher potential, where the generated pressure is proportional to the square of the electric field [14, 20].

## 3. Maximization of the Generated Pressure by an EHD Pump

Consider a pump unit that consists of pairs of two anodes and two cathodes. The dotted line in Fig. 3 shows one unit. For a constant applied voltage  $V$ , the pressure depends on  $r_1$ ,  $r_2$ , and  $d$ .

The ratio of variables to maximize the pressure induced by the unit length is estimated. Here, we consider a simple model of our EHD pump with interdigitated electrodes.

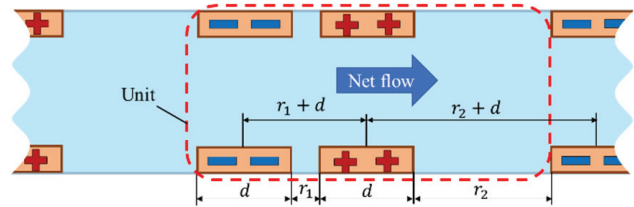


Fig. 3. Simple model of the electrode configuration.

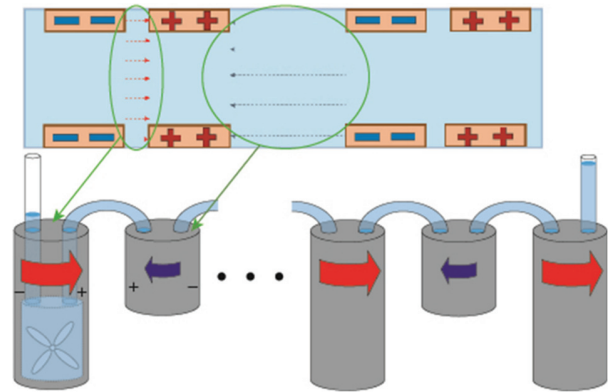


Fig. 4. Schematic of the pumping mechanism of an EHD pump.

The electric fields among the electrodes should generate the fluidic pressure when  $P(r_1)$  and  $P(r_2)$  are defined as the generated pressure at distances  $r_1$  and  $r_2$ , respectively. Fig. 4 shows the mechanism of our EHD setup where multiple pumps are connected in series.

Next, the pressure difference  $P_l$  between two edges of the unit is considered. Let  $E_1$  denote the strength of the uniform electric field formed between the cathode and anode, whose distance is  $r_1$ . Let  $E_2$  denote that between the anode and cathode belonging to the next unit, whose distance is  $r_2$ . The pressure difference  $P$  for a steady flow between two parallel electrodes induced by EHD is proportional to the squared electric field strength between the electrodes  $E^2$  [14].

Although the mechanism must be more complicated for the general arrangement of electrodes,  $P \propto E^2$  is often assumed and has been justified in the literature [14, 20]. Here, we assume that the contribution of electric fields formed between a pair of anodes is proportional to  $E_1^2$ , and the contribution of that for a pair of anodes next to a pair of cathodes is  $E_2^2$ :

$$P_l = A (E_1^2 - E_2^2), \dots \dots \dots (1)$$

where  $A$  is a constant that is independent of  $r_1$ ,  $r_2$ , and  $d$ . As the length of the unit is  $r_1 + r_2 + 2d$ ,  $E_1 = V/(r_1 + d)$ , and  $E_2 = V/(r_2 + d)$ , the average pressure difference per unit length  $\tilde{P}_l$  becomes

$$\begin{aligned} \tilde{P}_l(r_1, r_2, d) &= \frac{P_l}{r_1 + r_2 + 2d} \\ &= \frac{AV^2}{r_1 + r_2 + 2d} \left[ \frac{1}{(r_1 + d)^2} - \frac{1}{(r_2 + d)^2} \right]. \end{aligned} \quad (2)$$

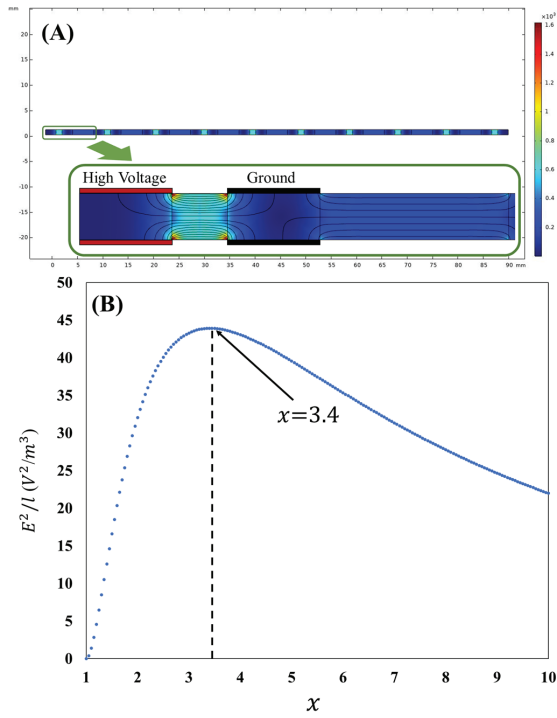


**Fig. 5.** Analysis result by the finite element method. (A) Electric field distribution. (B) Square of total electric field per total length vs.  $x$  position.

As  $\tilde{P}_l(r_1, r_2, d)$  is a monotonically decreasing function of  $r_1$  and  $d$ ,  $\tilde{P}_l$  becomes larger as  $r_1$  and  $d$  become smaller. On the other hand, there exists  $r_2 = r_2^*(r_1, d)$  that maximizes  $\tilde{P}_l$ .

From

$$\frac{\partial \tilde{P}_l}{\partial r_2} = 0, \dots \dots \dots (3)$$

we obtain

$$(r_1 + r_2^* + 2d)^2 (r_2^* - 2r_1 - d) = 0. \dots \dots \dots (4)$$

$$\therefore r_2^* = 2r_1 + d. \dots \dots \dots (5)$$

For technical reasons, a minimum value of  $d$  exists. Additionally, a minimum value of  $r_1$  exists to realize EHD phenomena. In our experiments, we set  $d = 2.0$  mm and  $r_1 = 1.2$  mm, leading to  $r_2^* = 4.4$  mm. The optimized ratio of  $x = r_2/r_1$  is  $x \simeq 3.7$ . In addition, we used the finite element method to analyze the EHD pump. After modeling the flow path and electrodes of the EHD pump, we analyzed the electric field when 1 kV is applied to the electrodes.

Figure 5(A) shows the result of the electric field analysis by COMSOL. Red and blue represent the electric field magnitude. Figure 5(B) shows the relation between the square of the total electric field per total length vs.  $x$  position obtained by the finite element method. Since the pressure generated by the EHD phenomenon is proportional to the square of the electric field, we speculated that the magnitude of the square of the electric field is comparable with the generated pressure. From these results, we

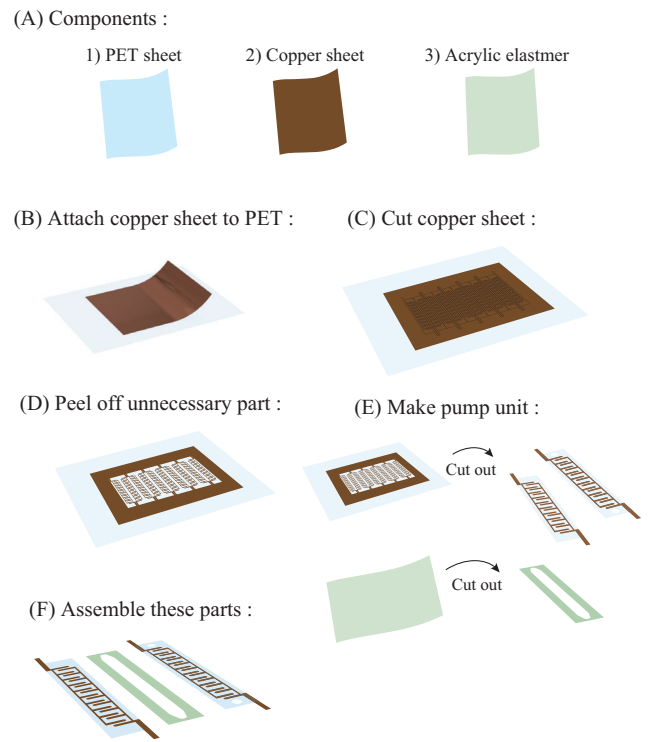


**Fig. 6.** Fabrication methods for a flexible EHD pump.

obtain  $r_2^* \simeq 4.1$  mm and  $x^* \simeq 3.4$ . The results show that the simple mathematical model generally agrees well with the finite element method.

### 4. Fabrication Methods

Figure 6 shows the fabrication methods of the flexible EHD pump. Figure 6(A) illustrates the three main components used for a flexible EHD pump. The exterior is composed of PP (polypropylene) sheets, while the electrodes are copper sheets with an adhesive layer. Copper, which has a high electric conductivity, is often used for electrodes of dielectric actuators. We used an adhesive acrylic elastomer (3M VHB4910J) for the middle layer because it provides excellent electric insulation and is compatible with the EHD pump.

Figures 6(B)–(F) illustrate how to process the materials. A copper sheet is initially attached on a PP sheet. Then a cutting plotter (GRAPHTEC CE6000-40 Plus) creates interdigitated incisions in the copper sheet. The excess parts are removed, and the copper sheet is cut into each unit with a laser cutter (TROTEC Speedy 100). Finally, the units are assembled to complete a flexible EHD pump.

Figure 7 shows the structure and photograph of a flexible EHD pump. The height of the pump flow channel should be small to increase the electric field density and generate high pressure. However, a lower height makes fluid flow difficult due to fluid effects, including the viscous resistance. In addition, optimizing the height of the flow channel is challenging because the flow rate must be

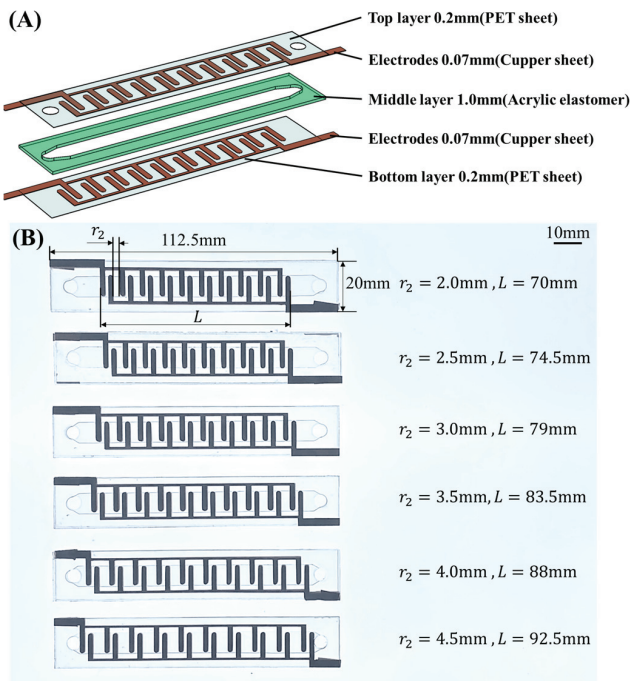


**Fig. 7.** Structure and photograph of flexible EHD pumps. (A) Structure of flexible EHD pump. (B) Photograph of six samples.

analyzed. Consequently, we set the height at 1 mm by referencing existing EHD pumps [14].

The above fabrication method can fabricate five pumps per hour. On the other hand, previous methods require time-consuming processes such as 3D printing and resin hardening [14]. They also require complicated fabrication processes and special materials [15, 21]. Therefore, this digital fabrication method is suitable to realize flexible and bendable EHD pumps. The pump is designed to be 1.2-mm thick with a weight of 2.1 g. Sequentially connecting multiple pumps can enhance the output pressure.

### 5. Experimental Setup

We prepared six pump samples with different electrode configurations in 0.5-mm intervals between 2.0 mm to 4.5 mm of  $r_2$  to identify the optimal electrode configuration of our flexible EHD pumps. To evaluate the performance of the pumps, the pressure, flow rate, and current were measured. We used Novec 7300 (3M) as a working fluid. Due to its excellent insulation and chemical stability, it is commonly employed as the working fluid for EHD pumps [22–24].

**Figure 8** depicts the experimental setup. We measured the pressure generated by our flexible EHD pump by connecting one side of the pump to a silicone tube and the other side to a pressure sensor (KEYENCE AP-10S) (**Fig. 8(A)**). The flow rate was evaluated by connecting silicone tubes to both sides of the pump and placing the flow rate sensor (KEYENCE FD-Xa1) between the tubes (**Fig. 8(B)**). The electric current was measured by con-

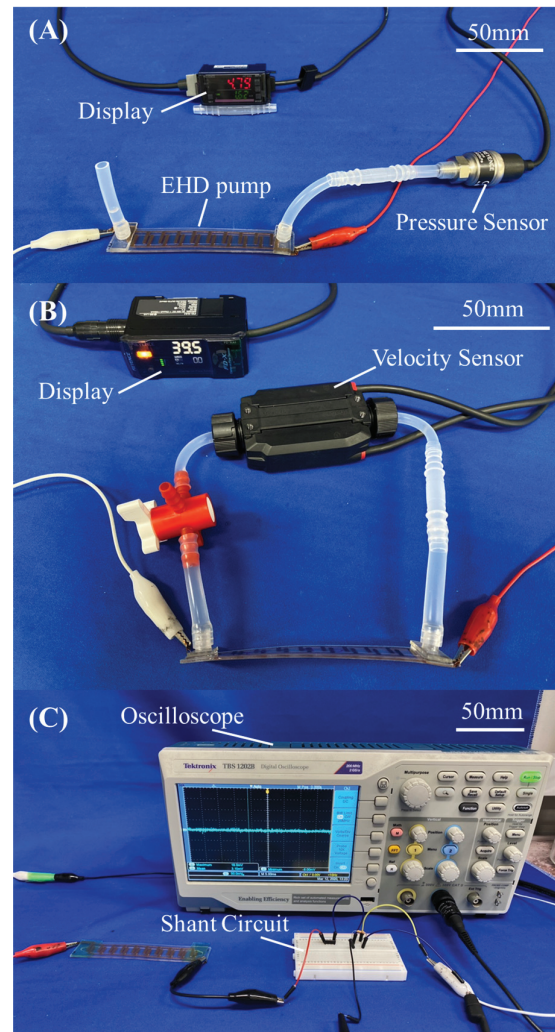


**Fig. 8.** Experimental setup. (A) Pressure measurement. (B) Flow rate measurement. (C) Current measurement.

necting the pump to the oscilloscope (**Fig. 8(C)**). When measuring the electric current, the pressure and the flow rate should be zero because both sides of the pump are sealed. However, the experimentally measured current values are almost coincident with one another. We calculated the power based on the measured current. We also compared the energy efficiency of the pump with other off-the-shelf fluid pumps. In each experiment, the input voltage was changed by 1-kV increments between  $-8$  kV and 8 kV to measure the pressure, flow rate, and current of the pumps. In addition, to evaluate the pump reliability, we fabricated five EHD pumps with the same electrode configuration ( $r_2 = 4.0$  mm) to compare the pressure and flow rate at a constant applied voltage of 8 kV.

### 6. Results

**Figures 9(A)–(G)** show the experimental results. **Fig. 9(A)** shows the relationship between the applied voltage and generated pressure. The generated pressure of

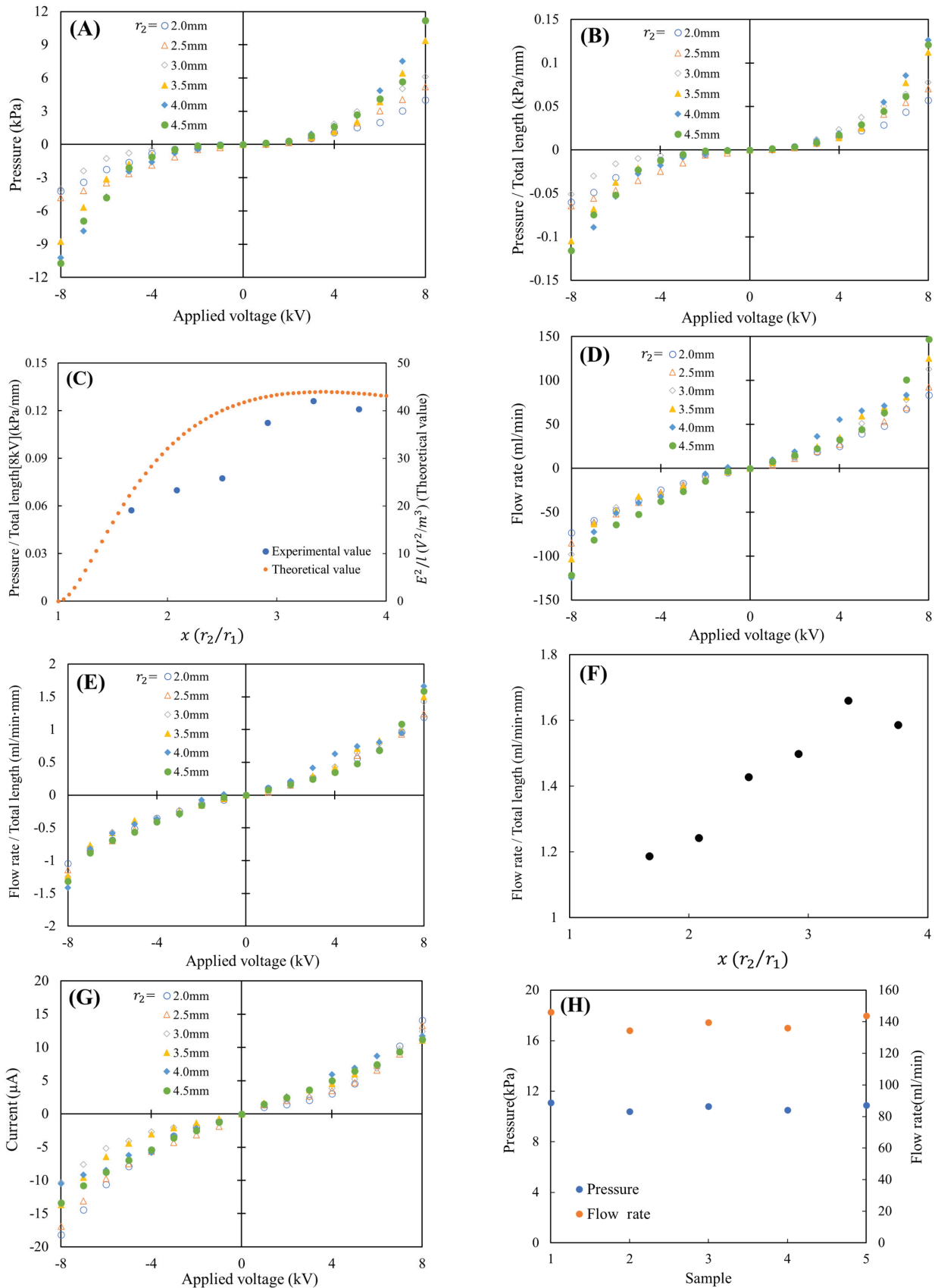


**Fig. 9.** Experimental results. (A) Pressure vs. applied voltage relation. (B) Pressure/total length vs. applied voltage relation. (C) Pressure/total length vs.  $x(r_2/r_1)$  relation. (D) Flow rate vs. applied voltage relation. (E) Flow rate/total length vs. applied voltage relation. (F) Flow rate/total length vs.  $x(r_2/r_1)$  relation. (G) Current vs. applied voltage relation. (H) Pressure and flow rate vs. 5 samples relation.

**Table 1.** Pump performances: miniature pump (TCS Micropumps, MGD1000S), large compressor (McMaster, single-tank portable air compressor).

	Mass [kg]	Power consumption [W]	Max pressure [kPa]	Max flow rate [mL/min]	Max pressure / W [kPa/W]	Max flow rate / W [mL/min·W]	Max pressure / mass [kPa/kg]	Max flow rate / mass [mL/min·kg]
Flexible EHD pump	0.0021	0.0936	11.1	146	118.6	1559.8	5285.7	69523.8
Miniature pump	0.142	30	800	500	26.7	16.7	5633.8	3521.1
Large compressor	15.422	1200	1034	42500	0.862	35.4	67	2755.8

our flexible EHD pumps increases with  $r_2$ . A maximum pressure of 11.2 kPa is generated by the pumps when  $r_2$  is 4.5 mm and 8 kV is applied. We assumed that increasing the distance between electrode pairs ( $r_2$ ) would decrease the reverse flow rate. **Fig. 9(B)** shows the relationship between the applied voltage and the generated pressure divided by the total length ( $L$ ) of the electrode units. A maximum is achieved when  $r_2$  is 4 mm ( $r_2/r_1 = 3.4$ ). **Fig. 9(C)** indicates the relationship between the generated pressure per unit length of the pumps and  $r_2/r_1$  when the applied voltage is 8 kV. The generated pressure per unit length is maximized at  $r_2/r_1 = 3.4$ . This behavior is consistent with the electric field analysis. Moreover, the maximum value of  $r_2/r_1 = 3.67$  approximately corresponds to the experimental results, demonstrating that the simple model of our flexible EHD pumps can optimize the electrode configuration. **Figs. 9(D)–(F)** depict the experimental results of the generated flow rate. As **Fig. 9(F)** shows, the flow rate is maximized when  $r_2/r_1 = 3.4$ . **Fig. 9(G)** depicts the relationship between the electric current and the voltage applied at each sample pump. When  $r_2$  is 4 mm and 8 kV is applied, the power consumption is 93.6 mW and the pressure generated per unit energy consumption is 118.6 kPa/W. This is the largest among the six samples. The results confirm that the electrode configuration can be optimized in terms of energy efficiency.

**Table 1** compares the pump performance with other off-the-shelf fluid pumps (miniature pump and large compressor). The output pressure per unit mass generated by our flexible EHD pump has a performance equivalent to the miniature pumps. Our proposed pump exhibits a higher performance in flow rate per unit mass, output pressure, and flow rate per unit consumption energy compared with the off-the-shelf pumps. **Fig. 9(H)** shows the relationship between the pressure and flow rate when applying 8 kV to 5 pumps with the same design. The pressure error and the flow error between the pumps are 3.4% and 4.4%, respectively. Hence, the fabrication method proposed in this study is reliable.

**Figure 10** shows that the flow meter can be rotated. In this research, we designed a circuit that can boost the voltage up to 8 kV with a DC/DC converter and general-purpose dry-cell batteries. Accordingly, our pump should realize a compact and portable system. Applying a voltage to the pumps rotates the flow meter counterclockwise (**Fig. 10(A)**). Upon reversing the wires, the fluid flows in the reverse direction, and the flow meter rotates

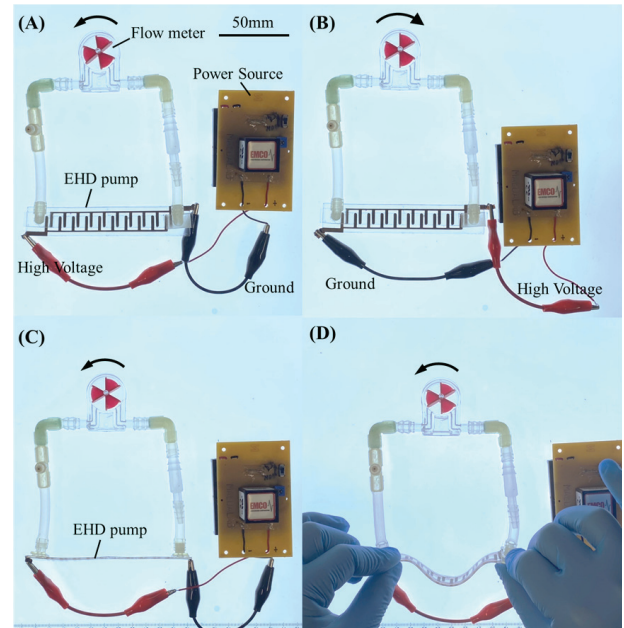


**Fig. 10.** Demonstration of a flexible EHD pump with a flow meter. (A) Basic setup. (B) Replaced wires. (C) Flat condition. (D) Bent condition.

clockwise (**Fig. 10(B)**). The flow meter keeps rotating (**Fig. 10(C)**) even if the pump is bent with an applied voltage (**Fig. 10(D)**). The flow rate of our flexible EHD pumps is 145 mL/min based on the number of flow meter rotations (53.1 rpm). This result is consistent with that in **Fig. 9(D)**.

The flow rate remains constant even when the EHD pump is bent. The result indicates that our flexible EHD pump has the potential to work even when deformed. Hence, the pump can be applied to wearable devices such as a smart textile [25] and an artificial hand [26]. Although our EHD pump requires a high voltage, it is safe for use in wearable devices. In the case of electricity, the parameter that affects people is not the voltage but the current. For example, the voltage of static electricity is about 4 kV, but static electricity does not hurt people. This is because its output current is negligible. Humans feel electricity at currents on the order of mA, but our pumps are driven by currents on the order of  $\mu A$  [27]. In addition, high-voltage-driven wearable devices that traditionally use electrostatic actuators have been proposed [28, 29].

## 7. Conclusion

Previous EHD pumps require complicated fabrication processes and special materials. Herein we report a process to easily and efficiently fabricate flexible EHD pumps. In addition, we propose a simple mathematical model to understand the EHD generated by interdigitated electrodes. The model agrees with the experimental results. These results suggest that the development of flexible EHD pumps for soft robots may realize a society where humans interact with machines.

### Acknowledgements

This work was supported by the Japan Society for the Promotion of Science [a Grant-in-Aid for Scientific Research on Innovative Areas (Research in a proposed research area) 18H05473; JRPs (Stretchable ElectroHydroDynamics)]. We also thank Dr. V. Cacucciolo and Prof. H. Shea for the assistance with EHD.

### References:

- [1] A. Minaminosono, H. Shigemune, Y. Okuno, T. Katsumata, N. Hosoya, and S. Maeda, "A deformable motor driven by dielectric elastomer actuators and flexible mechanisms," *Frontiers in Robotics and AI*, Vol.6, No.1, pp. 1-12, doi: 10.3389/frobt.2019.00001, 2019.
- [2] C. Jiang, K. Takagi, S. Hirano, T. Suzuki, S. Hosoe, K. Hashimoto, and A. Nozawa, "Flexible Parallel Link Mechanism Using Tube-Type Dielectric Elastomer Actuators," *J. Robot. Mechatron.*, Vol.27, No.5, pp. 504-512, doi: 10.20965/jrm.2015.p0504, 2015.
- [3] Y. Okuno, H. Shigemune, Y. Kuwajima, and S. Maeda, "Stretchable Suction Cup with Electroadhesion," *Advanced Materials Technologies*, Vol.4, No.1, 1800304, doi: 10.1002/admt.201800304, 2019.
- [4] S. Maeda, T. Kato, Y. Otsuka, N. Hosoya, C. Matteo, and C. Laschi, "Large deformation of self-oscillating polymer gel," *Physical Review E*, Vol.93, 010501, doi: 10.1103/PhysRevE.93.010501, 2016.
- [5] Z. Mao, M. Kuroki, Y. Otsuka, and S. Maeda, "Contraction waves in self-oscillating polymer gels," *Extreme Mechanics Letters*, Vol.39, 100830, doi: 10.1016/j.eml.2020.100830, 2020.
- [6] S. Maeda and S. Hashimoto, "Volume oscillation of microphase-separated gel," *Macromolecular Chemistry & Physics*, Vol.214, No.3, pp. 343-349, doi: 10.1002/macp.201200448, 2013.
- [7] H. Nakagawa, Y. Hara, S. Maeda, and S. Hashimoto, "A Pendulum-Like Motion of Nanofiber Gel Actuator Synchronized with External Periodic pH Oscillation," *Polymers*, Vol.3, No.1, pp. 405-412, doi: 10.3390/polym3010405, 2011.
- [8] H. Shigemune, S. Maeda, V. Cacucciolo, Y. Iwata, E. Iwase, S. Hashimoto, and S. Sugano, "Printed paper robot driven by electrostatic actuator," *IEEE Robotics and Automation Letters*, Vol.2, No.2, pp. 1001-1007, doi: 10.1109/LRA.2017.2658942, 2017.
- [9] H. Shigemune, S. Maeda, Y. Hara, N. Hosoya, and S. Hashimoto, "Origami Robot: A Self-folding Paper Robot with an Electrothermal Actuator Created by Printing," *IEEE/ASME Trans. on Mechatronics*, Vol.21, No.6, pp. 2746-2754, doi: 10.1109/TMECH.2016.2593912, 2016.
- [10] K. Suzumori, S. Iikura, and H. Tanaka, "Development of flexible microactuator and its applications to robotic mechanisms," *IEEE Int. Conf. on Robotics and Automation*, Vol.2, pp. 1622-1627, doi: 10.1109/ROBOT.1991.131850, 1991.
- [11] S. Kurumaya, H. Nabae, G. Endo, and K. Suzumori, "Design of thin McKibben muscle and multifilament structure," *Sensors and Actuators A: Physical*, Vol.261, No.1, pp. 66-74, doi: 10.1016/j.sna.2017.04.047, 2017.
- [12] S. Wakimoto and K. Suzumori, "Fabrication and basic experiments of pneumatic multi-chamber rubber tube actuator for assisting colonoscope insertion," *IEEE Int. Conf. on Robotics and Automation*, pp. 3260-3265, doi: 10.1109/ROBOT.2010.5509633, 2010.
- [13] V. Cacucciolo, H. Shigemune, M. Cianchetti, C. Laschi, and S. Maeda, "Conduction Electrohydrodynamics with Mobile Electrodes: A Novel Actuation System for Untethered Robots," *Advanced Science*, Vol.4, No.9, 1600495, doi: 10.1002/adv.201600495, 2017.
- [14] Y. Kuwajima, H. Shigemune, V. Cacucciolo, M. Cianchetti, C. Laschi, and S. Maeda, "Active suction cup actuated by Electro-HydroDynamics phenomenon," *IEEE/RSJ Int. Conf. on Intelligent Robots and Systems*, pp. 470-475, doi: 10.1109/IROS.2017.8202195, 2017.
- [15] V. Cacucciolo, J. Shintake, Y. Kuwajima, S. Maeda, D. Floreano, and H. Shea, "Stretchable pumps for soft machines," *Nature*, Vol.572, pp. 516-519, doi: 10.1038/s41586-019-1479-6, 2019.
- [16] H. Shigemune, S. Sugano, H. Sawada, S. Hashimoto, Y. Kuwajima, Y. Matsushita, S. Maeda, V. Cacucciolo, M. Cianchetti, and C. Laschi, "Swinging paper actuator driven by conduction electrohydrodynamics," *IEEE Int. Conf. on Robotics and Biomimetics*, pp. 379-384, doi: 10.1109/ROBIO.2017.8324447, 2017.
- [17] S. Yokota, K. Kawamura, K. Takemura, and K. Edamura, "High-Integration Micromotor Using Electro-Conjugate Fluid (ECF)," *J. Robot. Mechatron.*, Vol.17, No.2, pp. 142-148, doi: 10.20965/jrm.2005.p0142, 2005.
- [18] K. Tokida, A. Yamaguchi, K. Takemura, S. Yokota, and K. Edamura, "A Bio-Inspired Robot Using Electro-Conjugate Fluid," *J. Robot. Mechatron*, Vol.25, No.1, pp. 16-24, 2013.
- [19] P. Atten and J. Seyed-Yagoobi, "Electrohydrodynamically induced dielectric liquid flow through pure conduction in point/plane geometry-theory," *IEEE Trans. on Dielectrics and Electrical Insulation*, Vol.10, No.1, pp. 27-36, doi: 10.1109/TDEI.2003.1176555, 2003.
- [20] A. Ramos, "Electrokinetics and Electrohydrodynamics in Microsystems," Springer Science & Business Media, 2011.
- [21] Z. Mao, K. Yoshida, and J.-W. Kim, "Developing O/O (oil-in-oil) droplet generators on a chip by using ECF (electro-conjugate fluid) micropumps," *Sensors and Actuators B: Chemical*, Vol.296, No.1, 126669, doi: 10.1016/j.snb.2019.126669, 2019.
- [22] Y. Kuwajima, S. Maeda, and H. Shigemune, "Analysis of EHD pump with planer electrodes using FEM simulation," *Int. Symp. on Micro-NanoMechatronics and Human Science*, pp. 1-3, doi: 10.1109/MHS.2017.8305176, 2017.
- [23] T. Sato, Y. Yamanishi, V. Cacucciolo, Y. Kuwajima, H. Shigemune, M. Cianchetti, C. Laschi, and S. Maeda, "Electrohydrodynamic Conduction Pump with Asymmetrical Electrode Structures in the Microchannels," *Chemistry Letters*, Vol.46, No.7, pp. 950-952, doi: 10.1246/cl.170217, 2017.
- [24] T. Sato, S. Maeda, and Y. Yamanishi, "Study of Low Energy Micro EHD Pump by Designed Electric Field," *Int. Symp. on Micro-NanoMechatronics and Human Science*, pp. 1-3, doi: 10.1109/MHS.2018.8886968, 2018.
- [25] K. Cherenack and L. V. Pieterston, "Smart textiles: Challenges and opportunities," *J. of Applied Physics*, Vol.112, No.9, pp. 1536-1550, doi: 10.1063/1.4742728, 2012.
- [26] P. Polygerinos, Z. Wang, K. C. Galloway, R. J. Wood, and C. J. Walsh, "Soft robotic glove for combined assistance and at-home rehabilitation," *Robotics and Autonomous Systems*, Vol.73, pp. 135-143, doi: 10.1016/j.robot.2014.08.014, 2015.
- [27] R. M. Fish and L. A. Geddes, "Conduction of electrical current to and through the human body: a review," *Eplasty*, Vol.9, e44, 2009.
- [28] R. Hinchet, V. Vechev, H. Shea, and O. Hilliges, "DextrES: Wearable Haptic Feedback for Grasping in VR via a Thin Form-Factor Electrostatic Brake," *UIST '18: Proc. of the 31st Annual ACM Symp. on User Interface Software and Technology*, pp. 901-912, doi: 10.1145/3242587.3242657, 2018.
- [29] I. M. Koo, K. Jung, J. C. Koo, J. Nam, Y. K. Lee, and H. R. Choi, "Development of Soft-Actuator-Based Wearable Tactile Display," *IEEE Trans. on Robotics*, Vol.24, No.3, pp. 549-558, doi: 10.1109/TRO.2008.921561, 2008.



**Name:**  
Yumeta Seki

**Affiliation:**  
Department of Engineering Science and Mechanics, Shibaura Institute of Technology

**Address:**  
3-7-5 Toyosu, Koto-ku, Tokyo 135-8548, Japan

**Main Works:**  
• “Development of high pressure EHD pump using planer electrodes,” The Proc. of the Dynamics and Design Conf. 2019, 358, 2019 (in Japanese).

**Membership in Academic Societies:**  
• The Japan Society of Mechanical Engineers (JSME)

---



**Name:**  
Yu Kuwajima

**Affiliation:**  
Department of Engineering Science and Mechanics, Shibaura Institute of Technology

**Address:**  
3-7-5 Toyosu, Koto-ku, Tokyo 135-8548, Japan

**Brief Biographical History:**  
2019 Received Master degree from Shibaura Institute of Technology  
2019- BOSCH Co., Ltd.

**Main Works:**  
• “Stretchable pumps for soft machines,” Nature, Vol.572, pp. 516-519, 2019.  
• “Active suction cup actuated by ElectroHydroDynamics phenomenon,” IEEE/RSJ Int. Conf. on Intelligent Robots and Systems, pp. 470-475, 2017.

---



**Name:**  
Hiroki Shigemune

**Affiliation:**  
Department of Electrical Engineering, Shibaura Institute of Technology

**Address:**  
2018 Received Ph.D. degree from Waseda University  
2018-2019 Assistant Professor, Waseda University  
2019- Principal Investigator, Active Functional Device Lab., Shibaura Institute of Technology

**Brief Biographical History:**  
3-7-5 Toyosu, Koto-ku, Tokyo 135-8548, Japan

**Main Works:**  
• “Self-Assembled 3D Actuator Using the Resilience of an Elastomeric Material,” Front. Robot. AI, Vol.6, No.152, pp. 1-12, 2020.  
• “Printed paper robot driven by electrostatic actuator,” IEEE Robotics and Automation Letters, Vol.2, No.2, pp. 1001-1007, 2017.  
• “Origami robot: a self-folding paper robot with an electrothermal actuator created by printing,” IEEE/ASME Trans. on Mechatronics, Vol.21, No.6, pp. 2746-2754, 2016.

**Membership in Academic Societies:**  
• The Institute of Electrical and Electronics Engineers (IEEE)  
• The Japan Society of Mechanical Engineers (JSME)

---



**Name:**  
Yuhei Yamada

**Affiliation:**  
Department of Engineering Science and Mechanics, Shibaura Institute of Technology

**Address:**  
3-7-5 Toyosu, Koto-ku, Tokyo 135-8548, Japan

**Brief Biographical History:**  
2019 Received Ph.D. from Waseda University  
2019- Postdoctoral Researcher, Shibaura Institute of Technology

**Main Works:**  
• “Avalanche distribution of the fiber bundle model with random displacement,” J. Phys. Soc. Jpn., Vol.88, 023002, 2019.  
• “Condition of weak discontinuity for percolation models with edge selection rule depending on cluster sizes,” J. Phys. Soc. Jpn., Vol.87, 085002, 2018.

**Membership in Academic Societies:**  
• The Physical Society of Japan (JPS)  
• The Japan Society of Mechanical Engineers (JSME)

---



**Name:**  
Shingo Maeda

**Affiliation:**  
Department of Engineering Science and Mechanics, Shibaura Institute of Technology

**Address:**  
3-7-5 Toyosu, Koto-ku, Tokyo 135-8548, Japan

**Brief Biographical History:**  
2008 Received Ph.D. degree from Waseda University  
2005-2008 Research Assistant, Waseda University  
2008-2009 Assistant, Waseda University  
2009-2011 Assistant Professor, Waseda University  
2011-2014 Assistant Professor, Shibaura Institute of Technology  
2014- Associate Professor, Shibaura Institute of Technology  
2015-2016 Visiting Professor, The BioRobotics Institute, Scuola Superiore Sant’Anna

**Main Works:**  
• “Autonomous oil flow generated by self-oscillating polymer gels,” Scientific Reports, Vol.10, 12834, 2020.  
• “Stretchable pumps for soft machines,” Nature, Vol.572, pp. 516-519, 2019.  
• “Stretchable Suction Cup with Electroadhesion,” Advanced Materials Technologies, Vol.4, No.1, 1800304, 2019.

**Membership in Academic Societies:**  
• The Institute of Electrical and Electronics Engineers (IEEE)  
• The Robotics Society of Japan (RSJ)  
• The Japan Society of Mechanical Engineers (JSME)

---